Journal of Basic Physical Research ISSN: 2141-8403 Prints, 2141-8411 Online
Vol.14, Issue 1, March, 2025, pp. 109 – 117, Available online at https://journals.unizik.edu.ng/jbpr/

THE SUITABILITY OF ILLITIC CLAYS FROM LEKE-ONUEME SOUTHEASTERN NIGERIA FOR THE PRODUCTION OF DURABLE STONEWARE TILE CERAMICS

A.I. Omeokachie[1*], H.N. Ezeh[2], O.M. Nweke[3], E.O. Akpunonu[4], L.U. Onyeneke[5], C.J. Chizoba[6] and T.C. Azubuike[7]

[1.4]Department of Geological Sciences, Nnamdi Azikiwe University, Awka
[2]Department of Geology, Ebonyi State University, Abakaliki Ebonyi State, Nigeria
[3.5.6]Department of Geology and Geophysics, Alex Ekwueme Federal University, Ndufu Alike, Nigeria
[7]Department of Ceramic and Glass Technology, Akanu Ibiam Federal Polytechnic, Unwana Ebonyi State, Nigeria
**Corresponding author email: ai.omeokachie@unizik.edu.ng; Tel: +234(0) 8064640894*

Abstract
Illitic-rich clays, with their hygroscopic properties, are widely valued in brick-making and stoneware tile ceramics. This study investigates the mineralogical, geochemical, and technical properties of illitic-rich clays from Leke-Onueme, Southeastern Nigeria, as a viable raw material source. Technological tests, including firing linear shrinkage, water absorption, mass loss, bulk density, and flexural strength, were conducted on cylindrical specimens at temperatures ranging from 800 to 1000°C. XRD analysis revealed that the clays are interstratified with illite-kaolinite, containing significant amounts of quartz and minor flux-inducing minerals. Geochemical results indicated substantial SiO_2 (49.02-54.14%), Al_2O_3 (6.52-6.93%), and K_2O (1.02-1.41%) content, with a sum of exchangeable bases ($CaO+MgO+Fe_2O_3+Na_2O+K_2O$) between 15.84% to 19.77%, suggesting a high fluxing oxide content favorable for glassy phase formation and vitrification at lower temperatures. The clay workability chart confirmed acceptable extrusion characteristics, and organic matter content along with loss on ignition values were positive across samples. Mechanical strength improved notably with temperature due to dense, vitrified, and sintered microstructures facilitated by the fluxing action of minor oxides. Illite and kaolinite concentrations, alongside quartz content, contributed to the clays' firing behavior, promoting vitrification and hematite crystallization that resulted in coloration. The extensive analysis showed that the clays meet the American Society of Testing Materials (ASTM international) and Chinese standards for ceramic production. This also confirms their viability as high-quality raw materials for manufacturing of stoneware tiles, bricks, roof tiles, binders, and other structural components, indicating significant potentials in ceramic production.

Keywords: *Bricks, Clay Minerals, Earthenware Products, Stoneware Tiles Ceramics, Floor Tiles*

Introduction

Clays are very important in process industries, agriculture, engineering, environmental and miscellaneous applications. For centuries, clays served globally as major raw materials in industrial applications such as ceramics, earthenware products, tyres, papers as well as in petroleum industries (Diko-Makia and Ligege 2020; Revuelta 2021). They are generally considered to be < 0.002 mm in size (Semiz 2017). Presently, demands for clays as raw materials have risen sharply which could be attributed to the rapid increase in construction purposes owing to globalization and urbanization (Akintola *et al*, 2020).To continue in manufacturing ceramic products, and with the fact that clays as raw materials may become scarce in future (Terrones-Saeta *et al*, 2020) and considering that major countries like China, are already limiting their productions due to insufficient raw materials, there is an urgent need to source for cheap, locally available and sustainable materials that can meet the requirements of the raw materials (either raw or when beneficiated) to serve as alternative to the depleting natural resources.

Geographical Setting

The study area Leke-Onueme, a suburb of Neke community has a land coverage of about 8km^2 (Fig.1a). Their location coordinates within Neke area are (Lat.6°39$^{'}$ 57.25"-6^{0}48' 37.25" N and Long. 7° 39' 41.98" –7^{0}50$^{'}$56.98").

Leke -Onueme is in Isi Uzo Local Government Area of Enugu State. It shares a boundary on the east with Ado and Okpokwu of Benue State, Ishielu (L.G.A) of Ebonyi State, Akpoga-Imilike and Nike both in Enugu State. The study area is accessible through a network of major roads from Eha Amufu-Umuator-Agu-Udene road, Eha Amufu-Aguamede – Ikem road and Ikem – Mbu Roads.

Geological Setting

The study area lies within the Anambra Basin (Fig.1b). The basin, is part of Lower Benue Trough constituting major groups which are Eze-Aku Group as its oldest formation (Turonian) and Nkporo Group(Campano-Maastrichtian). The Anambra Basin is one of the seven sedimentary domains in Nigeria and covers an area of about 40000km^2 (Murat 1972; Nwajide 2006). Previous studies (Simpson, 1954; Reyment, 1965; Agumanu, 1989; Akande &Muche, 1989; Odoma *et al*., 2013) gave detailed accounts of the geology, stratigraphy, and economic potential of the Lower Benue Trough, Nigeria. The sediments were affected by the major Santonian folding and a minor Cenomanian folding and uplift (Murat,1972). Nkporo formation within the study area has clay facies occurring as massive interbeds and inter-stratified with ferruginized sandstone, shale, heterolith, lenticular and laminated beds.

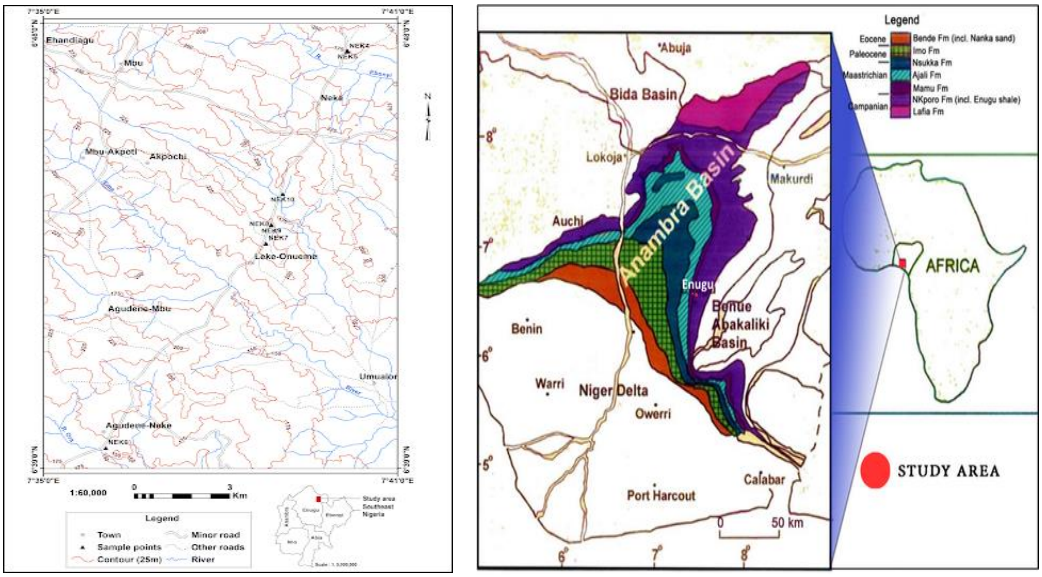

(a) (b)

Fig. 1: (a) Map of Leke-Onueme and its environs. (b) Regional stratigraphic map of Anambra Basin (adapted from Ogbahon and Olujinmi,2020) showing the Nkporo Formation where the study was carried out.

Materials and Methods

Sampling

Clay samples were collected from three different location points Nek.7(LO1), Nek.8(LO2), Nek.10(LO3) for laboratory analysis. The samples were packaged in separate polyethylene-bags, labeled with identification codes LO1 to LO3. The bags were later transported to the laboratory of University of Ilorin, Kwara State where sample preparations and laboratory testing on each of the clay samples commenced within 48 h of sampling. The samples were finally analyzed for various basic laboratory tests while specimen briquettes were molded for technological tests.

Preparation and Laboratory Testing

The grain size distribution analyses of the samples were performed by sedimentometry for particles of size ≤ 80 μm in accordance with D-422 ASTM standards. The fines fractions of the clay samples were characterized using hydrometer analysis that was based on Stokes law of sedimentation. The degree of plasticity of samples were achieved through the determination of Atterberg limits (liquid limit, LL and plastic limit, PL) using Casagrande apparatus in accordance with the ASTM-D4318 (2010) standards earlier described by Casagrande (1947). The mineralogical analyses on the powdered samples were carried out using the X-ray diffraction (XRD) and in accordance with that earlier described by Moore Duane and Reynolds Robert (1989). X-ray diffractograms were run under 3 treatments (natural, glycol and heated in 500°C for 4 h) ranging from 2° to 70° 2θ for bulk-sample diffractograms and from 2° to 40° 2θ for air-dried, ethylene-glycolated for 24 h, and heated to 550°C for 4 h for the clay proportions. Mineral identification from the diffractogram and a semi-quantitative mineralogical composition were carried out using earned value analysis (EVA) software.

X-ray fluorescence (XRF) spectrometer was used to determine the oxide of elements on the powdered form of the samples. The Philips PW 1600 X-ray spectrometer equipped with an end window 4 kW Rh anode X-ray tube was used. In order to study the evolution of firing properties of the samples, cylindrical samples were prepared. The samples were oven dried at 105°C for 24 h and grounded to a fine powder, then sieved using a mesh-size of 100 μm and were mixed with 26-28% water content to enhance particle binding in order to produce cylindrical shape. Then the wetted powdered samples were pressed under 150 kg/cm^2 pressure to obtain 100 × 50 × 8 mm prismatic samples. Then the samples were air dried for 24 h and oven dried at 105°C for 24 h to ensure that absorbed moistures were eliminated. After drying, the specimens were cooled in a drying room maintained at a temperature of 24°C, with a relative humidity between 30% and 70%. The specimens were therefore stored in the drying room at the required temperature and humidity until they were tested. Using a laboratory kiln, the dried samples were fired at different temperatures of 800°C, 900°C and 1000°C (in 100°C intervals) for a period of 5 h at a heating rate of 5°C/min using electrically powered laboratory furnace. A total of four tests were conducted per each property and the average results were tabulated.

Linear firing shrinkage (LFS) was calculated using the expression shown as follows

$$LFS\ (\%) = [(L0-L)/L0] \times 100 \quad (1)$$

This expression was according to the relative variation length of the briquette, where L0 represents the length of the briquette before firing and L represents briquette after firing.

Water absorption capacity (WA) was measured by weighing the fired briquette (M1) and the wet briquette (M2) after immersion in water for 24 h and was indicated with an expression as follows

$$WA(\%)=[M2-M1)/M1]\times 100 \quad (2)$$

Weight loss (WL) was calculated through the expression below

$$WL\ (\%) = [(M_d-M_f)/M_d] \times 100 \quad (3)$$

Where M_d represents the dry mass measured in g at 105°C and M_f represents the fired mass measured in g at each final firing temperature.

Bulk density (BD) of the briquette was represented in the equation (4) as

$$BD\ (g/cm^3) = M_f/V \quad (4)$$

Where Mf is the fired briquette weight measured in g and V represents the measured volume (cm^3) of the briquette.

The flexural strength (FS) of the samples was evaluated using three-point bending test method in accordance with ASTM F417-96 procedure. The value of modulus of FS for each of specimen was computed and recorded to the nearest 0.01 MPa with the expression represented as follows;

$$FS(MPa) = 3FL/2bd^2 \qquad 5$$

Where F = maximum load, L = distance between the supports (mm), b = net width of the specimen at the plane of failure (mm), and d = depth of the specimen at the plane of failure (mm). The data derived from the clays were fired at varying temperatures and the results were compared with standard specifications.

Results and Discussion

Compositions

The representative matched XRD patterns for the identified minerals are shown in Figures 2a andb. The prominent peak intensities at $2\theta=2.5^0$, $2\theta= 23.5^0$ and $2\theta = 24.5^0$ (2.5 Å and 3.4 Å) are characteristics of quartz. The presence of illites were indicated by the visible peak intensities at 2θ = 65.5 Å while kaolinite at 2θ = 51.5 Å and feldspars were identified at 2θ = 3.19 Å and 3.24 Å. From the semi-quantitative abundance of the identified minerals in the samples, the mineralogical compositions are summarized in Table 1. The XRD results revealed the predominance of clay minerals (illite-kaolinite) (42.26%) with high quantities of quartz content (54.14%) as well as considerable percentages of feldspar. The mineralogical classification of the samples revealed that one of the tested samples fell within roofing tiles region and structural clay products.

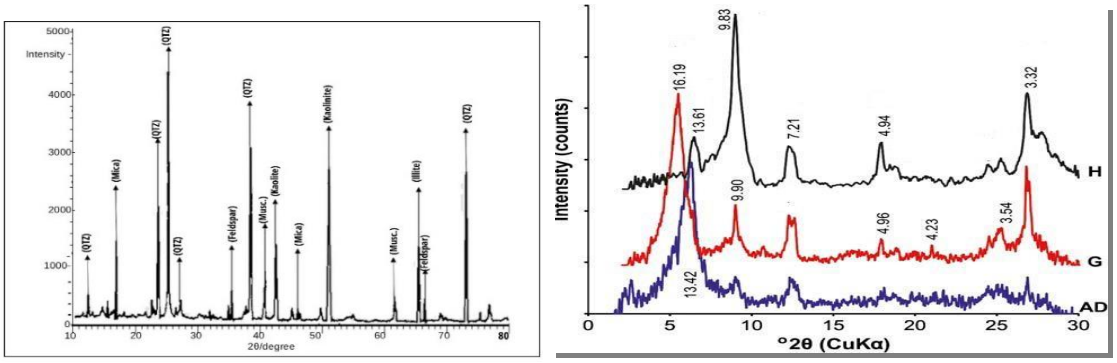

(a) (b)

*Fig. 2:(a) XRD analysis of the clays from Leke-Onueme, southeastern Nigeria, **(b).** Clay fraction of representative samples. Illite dominated in the left-hand patterns. Normal (H), glycolated (G), and heated at 550°C (AD).*

Table 1: Mineralogical composition of Leke-Onueme clays in weight percent

Whole Rock				**< 0. 002mm fraction**			
Sample ID	Quartz	Feldspar	Kaolinite	Illite	Muscovite	Mica	Clay Mineral
LO 1	53.13	4.16	21.09	6.09	6.96	8.12	42.26

The results of the chemical compositions as presented in Table 2 revealed the presence of major oxides with varying amounts of SiO_2 (49.02-54.14%) > Al_2O_3 (6.52-6.93%) > CaO (6.16-6.72%) > K_2O (1.02-1.41%) and > Na_2O (0.08-0.47%). The SiO_2/Al_2O_3 ratios ranging from 7.46 to 8.3 are higher than the values found in both pure kaolinite (SiO_2/Al_2O_3:1.18) and smectite (SiO_2/Al_2O_3:2.36) (Tsozue *et al*. 2017; Semiz and Celik 2020); a situation partly related to the high amount of free silica (quartz). According to Galan (2003), Na_2O_3 and K_2O are regarded as essential in production of roofing tiles as they act as fluxing agents thereby lowering the melting point of ceramic mixtures.

The fluxing agents such as alkali oxide ($Na_2O_3$and K_2O; 1.10-1.88%) was noted to be <4% whereas alkaline earth oxides (CaO and MgO; 6.74-7.99%) were noted to be generally > 4.0%, an indication of possible densification at high temperature. According to Dondi *et al*. (2002) and Semiz and Celik (2020), classifications based on Fe_2O_3 concentration of clay rich raw materials are as follows: (i) red firing clays, Fe_2O_3 concentration > 5%, (ii) tan-burning clays, Fe_2O_3 concentration between 1 and 5%, and (iii) white firing clays, Fe_2O_3 concentration < 1%. The Fe_2O_3 concentrations of the studied materials fell within the class of red firing clay materials. Based on chemical specifications, the concentrations of Al_2O_3, MgO and Fe_2O_3 for the studied clays are within the allowable parameters for ceramics formulations.

Table 2: Results of the chemical analyses (in wt %) of Leke-Onueme clays.

Sample Code	SiO_2	Al_2O_3	SO_3	Na_20_3	K_2O	CaO	MgO	TiO_2	P_2O_5	Fe_20_3	MnO	LOI	Total	Si/Al_2
LO1	54.14	6.52	0.05	0.05	1.36	6.16	1.18	0.7	0.17	9.57	1.25	4.26	85.41	8.30
LO2	54.10	6.93	0.07	0.08	1.41	6.72	1.27	0.67	0.19	9.90	1.34	6.39	89.07	7.81
LO3	49.02	6.57	0.07	0.47	1.02	6.42	0.58	1.03	0.05	8.00	0.56	5.43	79.22	7.46
Min	49.02	6.52	0.05	0.08	1.02	6.16	0.58	0.67	0.05	8.00	0.56	4.26		
Max	54.14	6.93	0.07	0.47	1.41	6.70	1.27	1.03	0.19	9.90	1.34	5.43		

Grain Size Distribution and Atterberg Limit

The results of the grain size distribution tests as presented in Table 3 revealed that the clay fraction (< 2 μm) ranged from 33.2% to 57.7%, the silt fraction (2 - 20 μm) ranged from 19.6% to 22.7% while the sand fraction (> 20 μm) ranged from 22.7% to 41.1%; an indication of the predominance of clay-silt materials.

Ekosse (1994), noted that high amounts of finer fractions of <2 μm, accounted for excessive shrinkage during firing which may not likely be the case with the study clays. The results of finer fractions of < 2 μm (33.2% to 57.1%) obtained can result in very low cracking due to shrinkage when fired for ceramic applications. To formulate ceramics bodies, Winkler Diagram was the tool used with the objective of obtaining products with good technological properties (Semiz 2017; Diko-Makia and Ligege 2020). With regards to Winkers diagram, the studied samples fell within roofing tiles and masonry bricks (Fig. 3). From the diagram, one sample plotted within the region of roofing tiles while the other two samples fell within the region of not suitable material.

The results of the Atterberg limits tests of the studied clays as presented in Table 3 revealed that liquid limit (LL) ranged from 32.2% to 61.2%, plastic limit (PL) ranged from 20.3% to 26.5% while the plasticity index (PI) ranged from 11.9% to 36.7%. The LL and PI values for the samples plotted on the Holtz and Kovacs (1981) diagram (Fig.4a) revealed that all the tested samples plotted in the medium to high plasticity region. From the diagram, the medium plasticity displayed by the studied samples showed consistency with predominant clay mineral being illite. The scattered plots in the Holtz and Kovacs diagram reveal that one of the samples fall within illite region, one within montmorillonite region with medium plasticity and these can be attributed to the abundance of fines fractions. The Casagrande (1948) chart (Fig. 4b)

revealed that the clays are generally of medium plasticity region, as they plot within the region of acceptable properties suitable for ceramic production.

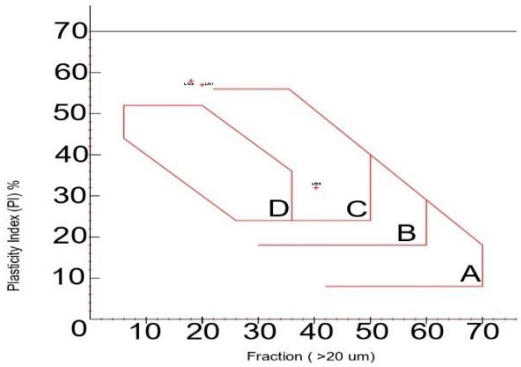

Fig. 3: *Grain-size distribution classification based on Winkler diagram for the technological classification of clay products (Winkler, 1954) and Diko-Makia & Ligege (2020). Fields are defined as: (1) common bricks, (2) vertically perforated/corrugated bricks, (3) roofing tiles and masonry bricks, and (4) perforated/hollow products.*

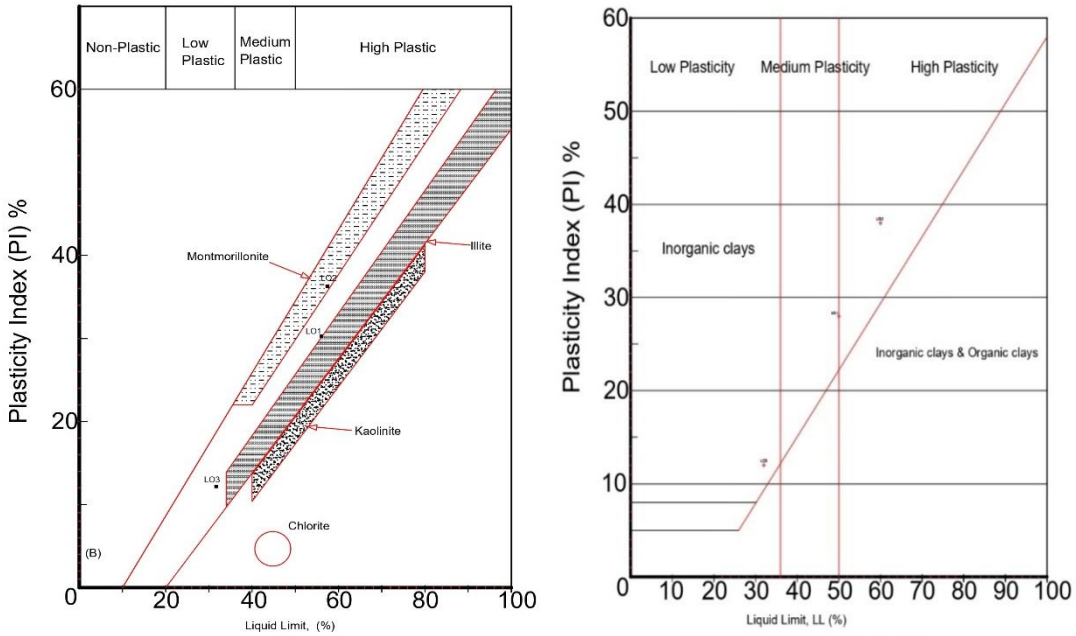

(a) (b)

*Fig. 4: Atterberg limits of the clays: **(a)** according to the Holtz and Kovacs (1981) diagram, **(b)** according to the Casagrande (1948) diagram*

Technological Properties of Leke-Onueme Clays

The results generated for linear firing shrinkage (LS) tests indicate that at 800°C, the linear firing shrinkage varied from 5.60% to 8.90% while at increased temperature of 1000°C, the LS varied from 10.4% to 15.3% (Table 4); an indication of increment with increased temperature. Linear shrinkage, according to Semiz and Celik (2020) gives an indication of the efficiency of firing and the acceptable values for aluminium silicates, kaolin and fired clays ranged from 7 to 10% (Diko-Makia and Ligege 2020).

Table 3: Results of the grain size distribution and Atterberg limit tests of Leke-Onueme clays

S/N	Sample ID	Grain size distribution			Atterberg limit		
		Clay (%) < 2 μm	Silt (%) 20-2 μm	Sand (%) > 20 μm	Liquid Limit %	Plastic Limit %	Plasticit y Index %
1	LO 1	57.1	20.2	22.7	55.3	26.5	28.80
2	LO 2	57.7	19.6	22.7	61.2	24.4	36.70
3	LO 3	33.2	22.7	41.1	32.2	20.3	11.90
	Min	33.2	19.6	22.7	32.2	20.3	11.90
	Max	57.7	22.7	41.1	61.2	26.5	36.70

Table 4: Results of technological properties tests at varying temperature.

Sample Code	Fired Temperature	Linear firing shrinkage %	Water absorption %	Bulk density g/cm^3	Weight loss %	Flexural strength (MPa)
LO 1	800 °C	5.60	20.99	2.19	10.44	2.69
	900°C	7.20	19.04	2.13	11.28	2.85
	1000 °C	10.4	17.60	2.09	12.29	3.02
LO 2	800 °C	8.10	21.06	2.08	9.83	2.31
	900°C	11.3	19.46	2.03	10.86	2.43
	1000°C	14.5	17.50	2.00	11.83	2.58
L0 3	800 °C	8.90	19.97.	2.18	10.00	2.01
	900°C	10.5	18.46	2.10	10.81	2.14
	1000°C	15.3	16.60.	2.08	11.98	2.26

Suitability of Leke-Onueme Clays as Raw Materials

The predominance of clayey-silt type materials favored them as good raw materials in ceramic bodies (Dondi 2001). The proportion of the clay fraction in a structural ceramic raw material is an indicator of plasticity and workability (Diko *et al*. 2011). The LL (32.2-61.2%), are in agreement with the range defined by Baccour *et al*. (2009) (30-60%) to the composition of raw materials used for ceramic production. From the Winkler's diagram, one of the samples plotted in the roofing tiles and masonry bricks domain while 2 plotted in region of not suitable material. From the chemical and mineralogical studies, the chemical results are consistent with mineralogical compositions which revealed the predominance of quartz, illite and Kaolinite with lesser amounts of feldspar and carbonate. Chemically, the major oxides present are SiO_2, Al_2O_3, Fe_2O_3 and CaO contents, with smaller quantities of Na_2O_3, K_2O, MgO, MnO, and TiO_2.The low WA recorded from the fired samples suggest low porosity which may likely results in no cracking of the finished products, thereby rendering them suitable for use in ceramic industry. For ceramic application, after firing to the temperature of about 1000°C, raw materials with FS ≥ 5.7 MPa with WA < 20% and WA < 25% (Onana *et al*. 2019) are considered valuable for roofing tile and dense bricks and ceramic blocks, respectively. Therefore, the fired temperature at about 1000°C can serve as most suitable condition for the beginning of liquid phase sintering, increased material densification and strength development of the raw materials. This is when we consider the fact that with high linear firing shrinkage values, deformation and microcracking are possible during the production of bricks.

Conclusions

Characterization of clays as raw materials in ceramic industry enabled the following conclusions to be drawn;

1. The clays classified predominantly as clayey-silt texture qualifies them for industrial ceramic applications. The mineralogy revealed the predominance of illite

and Kaolinite with high contents of quartz and feldspar and they greatly influence their development as ceramic materials.

2. During firing, at 800°C and above, results revealed an increase in the firing shrinkage and flexural strength with a decrease in WA values. Based on technological specifications, the materials revealed acceptable weight loss, linear firing shrinkage and water absorption with unsatisfactory performances for bulk density and flexural strength ($\leq$ 3.02 MPa) at fired temperature of 1000°C.
3. Knowledge of the technological properties of the clay samples revealed their possible utilization as raw material in industrial production of ceramic products and this will boost the nation's economy in terms of its gross domestic product and foreign exchange earnings.

References

Agumanu AE (1989). The Abakaliki and Ebonyi Formations: subdivisions of the Albian Asu River Group in the southern Benue Trough, Nigeria. Jour. African Earth Sciences, 9, pp. 195-207.

Akande, S.O and Muche, A (1989). Mineralogical, textural and Paragenetic studies of the lead-zinc-copper mineralization in the Lower Benue Trough (Nigeria) and their genetic implications. Journal of African Earth Sciences.9:445-456.

Akintola G.O, Amponsah-Dacosta F, Mhlongo S.E (2020). Geotechnical evaluation of clayey materials for quality burnt bricks, Heliyon 6 (12), e0562.

ASTM D-422 Standards: A standard test method for particle size analysis of soils.

ASTM D4318 (2010). Standard test methods for liquid limit, plastic limit, and plasticity index of soils. ASTM International, West Conshohocken.

ASTM F 417-96: Standard test method for flexural strength (modulus of rupture) of electronic-grade ceramics.

Baccour H, Medhioub M, Jamoussi, Mhiri T (2009). Influence of Firing Temperature on the Ceramic Properties of Triassic Clays from Tunisia. Jour, of Mater. Proc Tech. 209, 2812-2817.

Casagrande A (1947). Classification and identification of soils: Am. Soc. Civil Engineers Proc., 73(6) pt.1, P. 783 – 810.

Casagrande A (1948). Classification and identification of soils. Transaction of the American Society of Civil Engineers, 113, 901-930.

Diko ML, Ekosse GI, Ayonghe S, Ntasin. (2011). Physical characterization of clayey materials from tertiary volcanic cones in Limbe (Cameroon) for ceramic applications. Appl. Clay Sci., 51, 380–384.

Diko-Makia L, Ligege R. (2020). Composition and Technological Properties of Clays for Structural Ceramics in Limpopo (South Africa). Mi*nerals* 2020, *10*(8), 700 Dondi M (2001). Technological and compositional requirements of clay materials for ceramic tiles. Proceedings of the 12th International Clay Conference - Bahía Blanca, Argentina, July 22-28, 2001 - Eduardo A. Domínguez, Graciela R. Mas, Fernanda Cravero (Editors), 23-30.

Dondi M, Ercolani G, Guarani G, Raimondo M (2002). Orimulsion fly ash in clay bricks. Part 1: Composition and thermal behavior of ash. J. Eur. Ceram. Soc., 22, 1729–1735.

Dondi M (2001). Technological and compositional requirements of clay materials for ceramic tiles. Proceedings of the 12th Inter. Clay Confer. Bahia Blanca, Argentina, July 22-28,2001. Eduardo A.,Dominguez,Graciela R., Mas,F.C (editors), 23-30.

Ekosse G (1994). Clays: a gateway into the future. Botsw. Notes Rec. 26, 139-149.

Galan H.E (2003) Mineralogia Aplicada. 1st ed. Madrid: Sintesis, 399 p.

Holtz RD, Kovacs WD (1981). An Introduction to Geotechnical Engineering; Prentice-Hall, Inc.: Upper Saddle River, NJ, USA, 853p.

Moore Duane M, Reynolds Robert Jr. C (1989). X-ray Diffraction and the identification and analysis of clay minerals. Oxford University Press, Oxford, 25, 543-545.

Onana V.L, Ntouala R.F.D, Mbey J.A, Ngo'o Ze A, Kabeyene V.K, Ekodeck G.E (2019). Mineralogy and preliminary assessment of the potential uses of alluvial clays from Batouri (Eastern- Cameroon), Cerâmica 65: 407-415.

Revuelta M.B (2021). Construction materials; Geology, Production and Applications. Springer nature Switzerland AG.

Semiz B (2017). Characteristics of clay-rich raw materials for ceramic applications in Denizli region (Western Anatolia). Appl. Clay Sci. 2017, 137, 83–93.

Semiz B, Çelik S.B (2020). Mineralogical and geochemical characteristics of Belevi clay deposits at Denizli, SW Turkey: industrial raw material potential, Arabian Jour. of Geosciences 13:313.

Tsozue D, Nzeukou N.A, Mache J.R, Loweh S, Fagel N (2017). Mineralogical, physico-chemical and technological characterization of clays from Maroua (Far-North, Cameroon) for use in ceramic bricks production. J. Build. Eng. 11: 17–24.

Winkler H.G.F (1954) Bedeutung der Korngrossenverteilung und des Mineralbestandes von Tonen fur die Herstellung grobkeramischer Erzeugnisse. Ber Dtsch Keram Ges 31:337–343

Odoma, A.N., Obaje, N.G., Omada, J.I., Idakwo, S.O., Erbacher, J. (2013). Paleoclimate reconstruction during Mamu (Cretaceous), Based on Clay Mineral Distributions. *J. Appl. Geol. and Geophysics*. 1(5): 40 – 46.

Murat, R.C. (1972). Stratigraphy and Paleogeography of the Cretaceous and Lower Tertiary in Southern Nigeria, In: Dessauvagie, T.F.J., Whiteman, A.J. (Eds) African Geology. Geology Dept. Univ. Ibadan, Nigeria.

Nwajide, C.S. (2006). A guide for geological field trips to Anambra and related sedimentary basins in southeastern Nigeria. Petroleum Technology Development Fund (PTDF) chair in Geology, Great AP Express Pub. Ltd, Nsukka.

Reyment, R.A. (1965). Aspects of the Geology of Nigeria: The stratigraphy of the Cretaceous and Cenozoic Deposits. Ibadan University Press. 145p.

Simpson A (1954). The Nigerian Coal Field: The geolgy of parts of Onitsha, Owerri and Benue provinces. Geological Survey Nigeria Bull. 21:1-67

Terrones-Saeta J.M.,Suarez-Macias J.,Iglesias-Godino F.J and Corpas-Iglesias F.A (2020). Study of the Incorporation of Biomass Bottom Ashes in ceramic Materials for the manufacture of Bricks and Evaluation of their Leachates. Materials, 13,2099.

Tsozue D., Nzeukou N.A.,Mache J.R.,Loweh S and Fagel N (2017). Mineralogical, physic-chemical and technological characterization of clays from Maroua (Far-North, Cameroon) for use in ceramic bricks production. J.Build.Eng.11:17-24.

Winkler H.G.F (1954). Bedeutung der korngrossenverteilung und des Mineralbestandes von Tonen fur die Herstellung grobkeramischer Erzeugnisse. Ber Dtsch Keram Ges 31:337-343.